

XIII International Conference on Computational Plasticity. Fundamentals and Applications
COMPLAS XIII
E. Oñate, D.R.J. Owen, D. Peric and M. Chiumenti (Eds)

INFLUENCE OF INTERFACE ZONE BEHAVIOUR IN REINFORCED CONCRETE UNDER TENSION LOADING: AN ANALYSIS BASED ON MODELLING AND DIGITAL IMAGE CORRELATION

N. HANDIKA*, G. CASAUX-GINESTET* AND A. SELLIER*

*Laboratoire Matériaux et Durabilité des Constructions (LMDC)
Université de Toulouse ; UPS, INSA ; LMDC
135, Avenue de Ranguel, 31077 Toulouse Cedex 04, France
E-mail: handika@insa-toulouse.fr - Web page : <http://www-lmdc.insa-toulouse.fr/>

Key words: Reinforced Concrete, Interface Zone, Modelling, Digital Image Correlation.

Abstract. The problem of durability in reinforced concrete structures is a major case of concern nowadays. The problem of leakage due to cracking phenomena in critical structures such as nuclear power plants is specifically significant. In these structures, the number of cracks, their distribution and opening are needed to predict leakage possibilities. These variables depend on both the behaviour law of concrete and the behaviour law of steel-concrete interface.

This article intends to compare experimental and modelling results focusing on interface zone between concrete and steel reinforcement. The first step consists in performing tests to capture behaviour of reinforced concrete prismatic elements subjected to pure tension. Crack opening along these structures is investigated by using digital image correlation (DIC), which allows the observation of crack propagation during loading.

Next, the tension test of reinforced concrete is modelled in two different ways. Firstly, the connection zone between concrete and steel bar is assumed to be perfect (none-sliding connection). Then, a hypothesis of interface zone model between these two materials which allows plastic sliding [1], is considered. An orthotropic model of concrete based on plasticity and damage theories is used for this modelling. The model is able to predict crack opening and manage its reclosure [2]. Finally, results of the test are compared to the both modelling. A discussion concerning the need of interface model finishes this paper.

1 INTRODUCTION

The French National research project for design and assessment of special concrete structures ([PN CEOS.fr](http://pn.ceos.fr)) has objective to understand and control the problem of cracking [3]. The phenomenon of crack in a case of nuclear power plants buildings can lead to potential leakage problems of structures. In this condition, the number of cracks, their distributions and opening are specifically significant to predict as evaluation term. These variables depend on both the behaviour law of concrete and the behaviour law of steel-concrete interface. Characterizing the crack opening in reinforced concrete structures using finite element analysis appears as an interesting alternative to predict its mechanical behaviour.

The main objective of this works is to compare experimental and modelling results of crack opening focusing on interface element between concrete and steel reinforcement up to certain value of applied force. Due to the presence of ribs in high resistance steel bar and some concrete volume between its ribs, a zone called interface is usually defined. As steel reinforcement bar is loaded under tension, interface between steel and concrete transfer the stress from steel bar to concrete massif volume. During the loading process, different behaviour occurs in this zone comparing to the massif concrete part [1,4]. Some studies based on experimental results and modelling show the importance to distinguish these interface elements from concrete and steel in reinforced concrete structures [4,9].

The first part of this work consists in performing tests to capture behaviour of reinforced concrete prismatic elements subjected to pure tension loading using digital image correlation (DIC). In the second part, tension test is modelled by taking into account two different conditions. Firstly, a none-sliding connection between concrete and steel bar is assumed. This model is called Perfect Interface. Secondly, the hypothesis of plastic sliding between concrete and steel bar [1] is applied in the interface zone (Sliding Interface). Both model use an orthotropic behaviour law for plain concrete, developed in LMDC. Results of the experimental test are compared to the both modelling. A discussion regarding the necessity of interface model concludes this paper.

2 EXPERIMENTS USING DIGITAL IMAGE CORRELATION ANALYSIS

The best adapted test to observe the propagation of crack in reinforced concrete structures is a tensile test of simple prismatic element with one reinforcement bar in the centre of the concrete volume; Figure 3 shows the detail specification of this specimen. As the specimen is subjected to pure tension loading, the effects of steel and concrete bond such as stress redistribution, tension stiffening reduction and forces concentration in some local points can be observed [4]. DIC is used to observe the appearance of crack on the surface of concrete. Table 1 describes the materials used and the condition of concrete conservation. Evidently, some primary tests are required to characterize the materials and local behaviour law of interface element. Table 2 and 3 describe the mechanical properties of concrete and steel bar reinforcement.

Table 1: Mixed-design of concrete materials

Type of concrete	C35/45 XF1 normal concrete, exposures classes according to Eurocode 2: Moderate water saturation without de-icing agent [8].
W/C	0,6
Type of sand	0/4 mm (830 kg/m ³) - natural sand silico-calcaire
Type of aggregates	4/11 mm (445 kg/m ³) - natural aggregates silico-calcaire
	8/16 mm (550 kg/m ³) - natural aggregates silico-calcaire
Type of Cement	CEM I 52.5 N CE CP2 (320 kg/m ³) (High resistance Portland cement for aggressive environments)
Admixture	Superplasticizer Sikaplast Techno 80 based on modified polycarboxilates (2.4 kg/m ³)
Conservation of concrete	Conservation room maintained at 20°C and 100% of relative humidity

Table 2: Mechanical properties of concrete

Compressive strength*	$R_c = 56.57$ MPa
Tensile strength* (Brazilian test)	$R_t = 3.95$ MPa
Modulus of elasticity*	$E = 38\,500.00$ MPa

* Measured average value of experimental results at 126 days of concrete casting

Table 3: Mechanical properties of steel bar

Fe E 500 HLE (<i>Haute Limite Elastique</i> – High Strength Steel)	
Nominal diameter of HA steel bar	$\phi = 12.00$ mm
Yield strength*	$f_y = 566.0$ MPa
Modulus of elasticity*	$E = 185.9$ GPa

* Measured average value of tensile test result of steel reinforcement bar

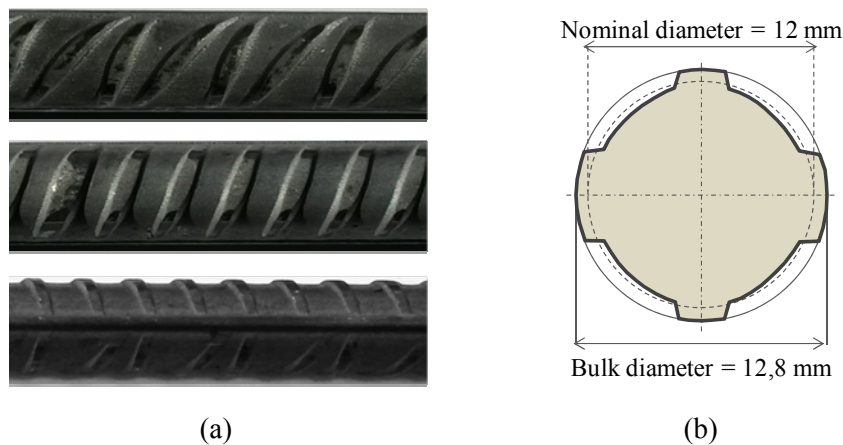


Figure 1: Surface geometry of steel reinforcement bar
 (a). Reinforcement bar in LMDC. (b). Illustration of reinforcement bar with its ribbed section [5].

The nominal bar diameter is 12 mm, it has a section of 113 mm^2 [5]. Observing the steel reinforcement bar used in this study, as presented in Figure 1, there are two different ribs motifs, one for each side. This condition recalls the asymmetrical geometric of reinforcement bar which will be neglected in the model. However, it could explain a part of the asymmetry of the experimental crack propagation.

A pull-out test was carried out with the purpose of determining the adhesion of concrete and reinforcement bar. Conforming to RILEM [6], five times diameter of the bar is the effective encasement height of the bar inside the concrete volume. Two ends of the bar inside the concrete are protected by PVC pipes to reduce the influence of disturbed area and localize the shear stresses along a relative short zone [6]. Experimental results and details of specimen of this test are shown in the Figure 2 below. The maximum shear stress attained is 20.56 MPa. This shear stress is a mean value along the cohesion zone.

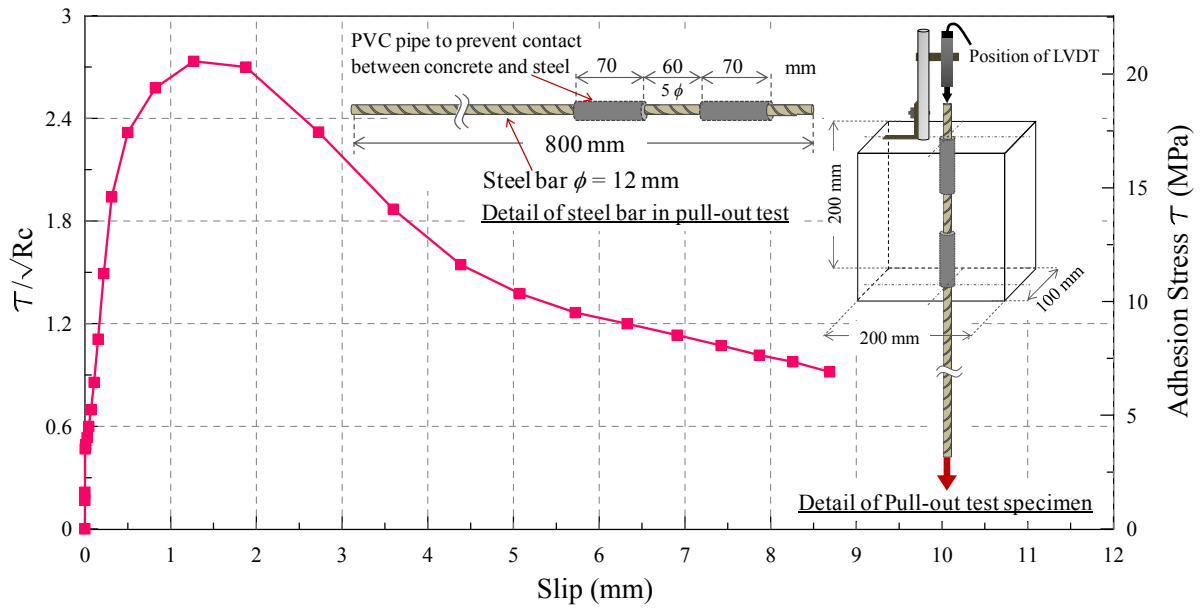


Figure 2: Pull-out test: experimental results and details of specimen.

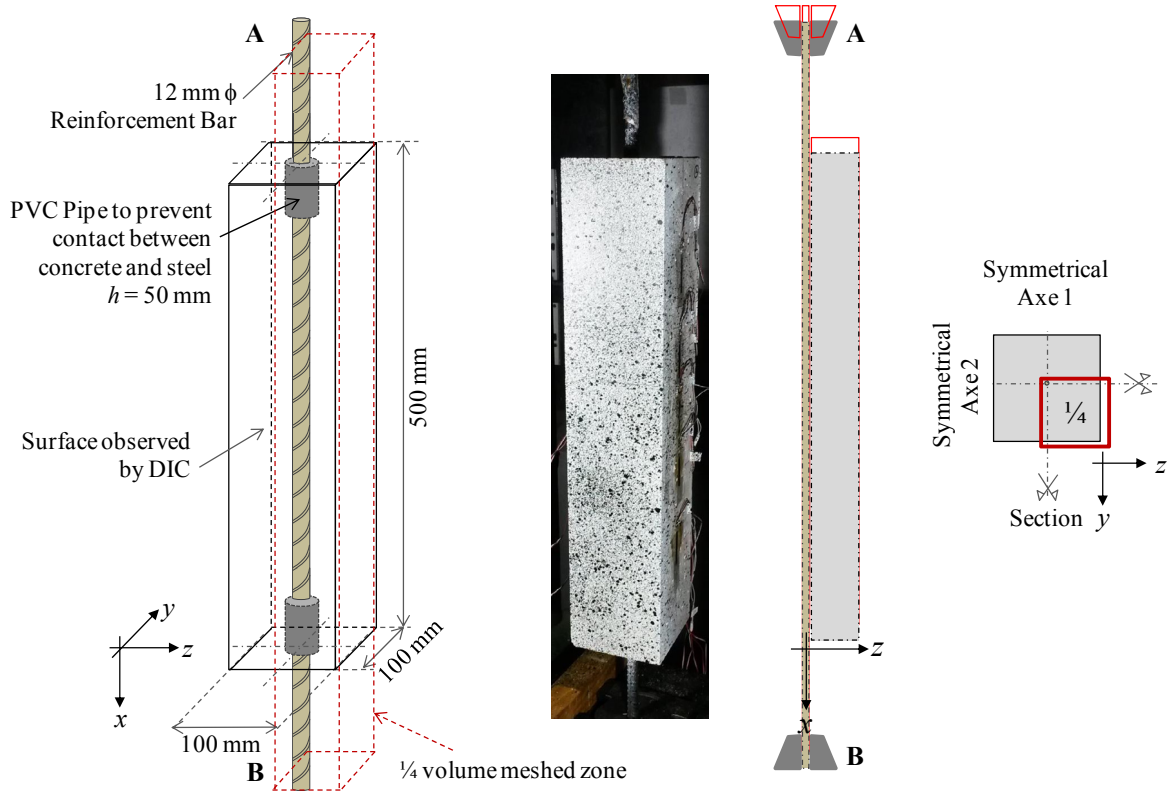


Figure 3: Dimension of concrete tensile test specimen.

After knowing the characteristics of concrete and interface element, tensile tests of simple

prismatic element were carried out. One high resistance reinforcement steel bar with 12 mm of nominal diameter is casted. Same as the pull-out specimen, at two ends of concrete, the bar is covered by PVC plastic pipes to prevent contact steel-concrete during casting, and consequently, to avoid spall off concrete during the loading (detailed specification is shown in Figure 3). Ten centimetres long of steel bar separated the concrete part in two ends from the grip of tension loading machine. One far end B is kept steady while the other end A is charged in imposed displacement of 1.8 mm/minute.

3 NUMERICAL MODELLING OF REINFORCED CONCRETE

The numerical simulations, which were carried out within the context of this study, have been made by using Finite Element code CAST3M [7]. As two different conditions are considered in modelling works (non-sliding hypothesis and plastic sliding hypothesis between concrete and steel reinforcement bar), the three behaviour laws used in the model are presented in this part: concrete, steel bar reinforcement and steel-concrete interface elements. The perfect interface model uses the behaviour of concrete in its interface zone while the sliding interface model applies plastic sliding hypothesis between bar and plain concrete.

3.1 Behaviour law of plain concrete [2]

A three dimensional formulation of orthotropic damage is used to model the plain concrete. The LMDC concrete model is based on a coupling of plasticity with damage theory. Therefore, it is able to be combined with other aspects of concrete structure behaviour, such as shrinkage and creep behaviour [2]. Taking into account the crack-reclosure process, this model is illustrated in Figure 4, with a curve of uniaxial cyclic test (several cycles in tension followed by a simple compression).

Under tension loading, after reaching its peak point in stress-strain curve, a localized damage D^t allows a decreasing in stiffness. As cracks propagate perpendicularly to the effective tensile principal stress, an orthotropic Rankine multi-criterion is used (three orthogonal tensile principal stresses). During crack reclosure, as soon as a contact between two cracked surfaces occurs, due to unloading or compressive loading, a compressive stress $\tilde{\sigma}^f$ is assumed created between the two rough boards of the crack. This compressive stress governs the reclosing of the crack, as in the Jefferson et al.'s model [11].

In the undamaged zone, $(1 - D^t)$, subsists an effective stress $\tilde{\sigma}^h$, while another stress $\tilde{\sigma}^f$ corresponds to the reclosure action in the cracked zone D^t . Concerning tensile damage, its evolution law is regularized using an accurate procedure based on an anisotropic Hillerborg method [12] Interaction between these two stresses and damage tensors leads to a resulting stress $\tilde{\sigma}^c$. This stress is able to reach another criterion: the Drucker Prager ones, causing shear damage, D^c , able to consider softening possibility in compression as illustrated in Figure 4. Finally, Equations (1) and (2) resume the different aspects of this concrete behaviour law.

In this article, for modelling the two conditions mentioned in the beginning, the value of fracture energy (G_{ft}), which was not measured, was chosen as proposed by Ottosen's equation [10], leading to a value of 154 J/m².

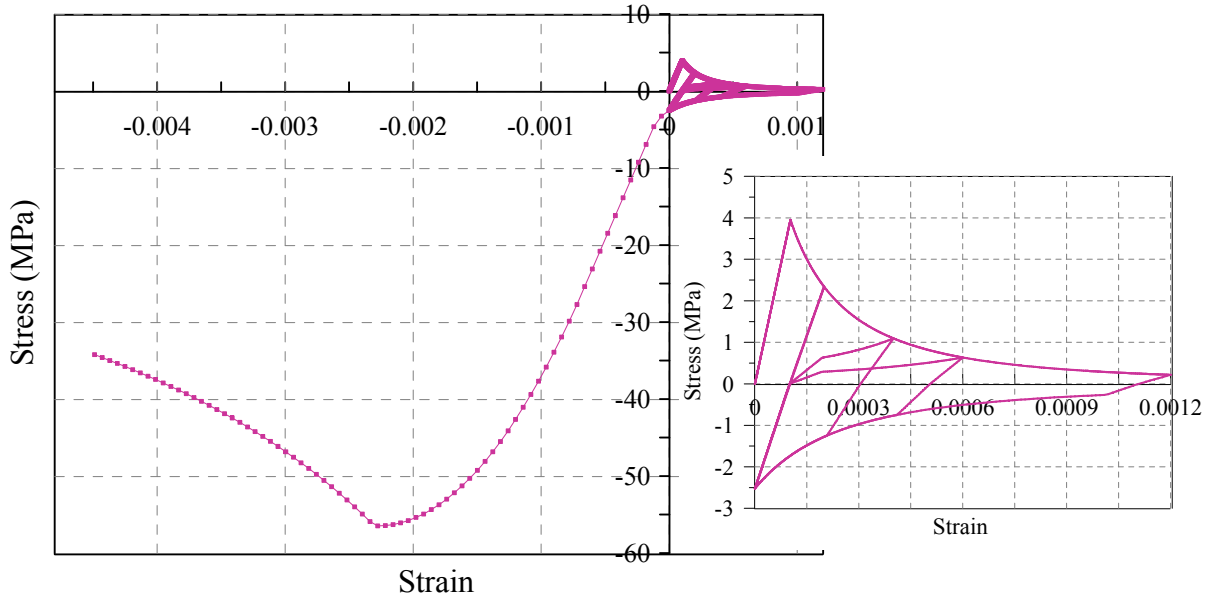


Figure 4: Stress-strain curve in cyclic tests of model LMDC.

$$\vec{\sigma} = (1 - D^c) \underbrace{\left((1 - D^t) \vec{\sigma}^h + D^t \cdot \vec{\sigma}^f \right)}_{\vec{\sigma}^c} \quad (1)$$

$$\vec{\sigma} = (1 - D^c) (1 - D^t) S^0 \cdot \vec{\varepsilon} + (1 - D^c) D^t \cdot S^0 \cdot (\vec{\varepsilon} - \vec{\varepsilon}^f) \quad (2)$$

In equation (1) and (2), the notation system is the pseudo vector ones, in which the symmetric stress tensors are stored as 6 components vectors.

Where:

- $\vec{\sigma}$ = Apparent stress
- $\vec{\sigma}^h$ = Concentrated stress in undamaged zone $(1 - D^t)$
- $\vec{\sigma}^f$ = Reclosure stress in damaged zone D^t
- $\vec{\sigma}^c$ = Compressive stress resulting from interaction of two stresses $\vec{\sigma}^h$ and $\vec{\sigma}^f$ in damaged and undamaged zone
- D^t = Tensile damage tensor
- D^c = Compressive damage tensor
- S^0 = Stiffness matrix of material, second order tensor
- $\vec{\varepsilon}$ = Strain pseudo vector
- $\vec{\varepsilon}^f$ = Un-elastic strain in the damaged part of material

3.2 Behaviour law of steel reinforcement bar

Steel reinforcement bar is modelled as mechanic elasto-plastic perfect. Based on the

experimental tensile test result, the steel bar reached the yield strength of 567.30 MPa at 0.37% of strain and 185.9 GPa of Young's modulus.

3.3 Behaviour law of plastic sliding interface zone

The interface zone thickness is taken arbitrarily at 3 mm, greater than steel bar ribs and smaller than characteristic dimensions of the element, also to facilitate the meshing in finite element model (as illustrated in Figure 5 and Figure 6). In the Figure 5, the equivalent uniaxial behaviour law of plastic sliding interface used in FEM is shown. In this figure, experimental curve is compared with an Eligehausen's model (fitted on experimental results) and used as hardening-softening law with a von Mises criterion for the massive element corresponding to the interface zone.

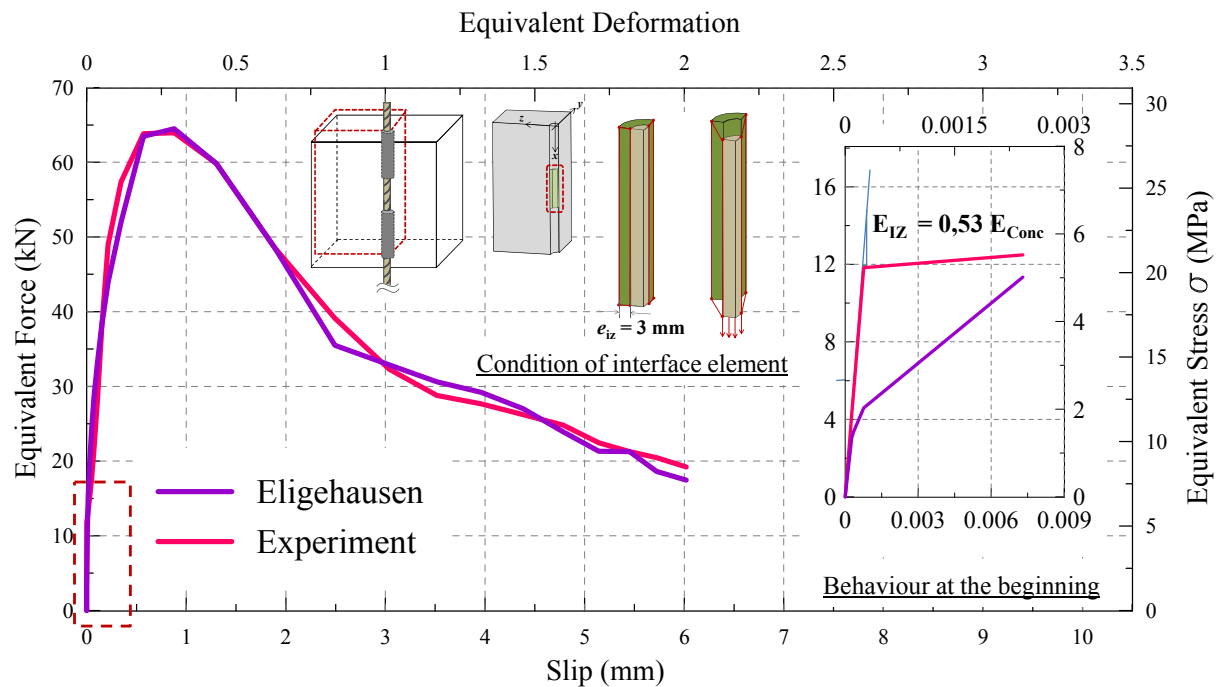


Figure 5: Equivalent uniaxial behaviour law of plastic sliding interface: experimental results and Eligehausen's model.

3.4 Modelling

The finite element mesh used for the numerical simulations is presented in Figure 3 and 6. Taking advantage of its two symmetrical axes, a quarter of the specimen is discretized with CUB 8 elements. Details of boundary conditions and meshing are presented. In order to understand the behaviour of nearly equal form of interface element, steel bar reinforcement is meshed in 3D. A quarter tube form of interface element is obtained (in green colour).

As mentioned before, two conditions of modelling are successively envisioned. For the first model, named *Perfect Interface* (PI), as a none-sliding connection between concrete and steel bar is assumed, only the behaviour of concrete model is used (poisson's ratio $\nu = 0,2$). For the second model, named *Sliding Interface* (SI), as the hypothesis of plastic sliding between concrete and steel bar is considered, the plastic sliding interface model is applied in

the interface zone. Coefficient of poisson's ratio $\nu = 0$ is then used to limit Poisson's effect which could lead to damage prematurely of concrete elements in contact with interface elements. Experimental and modelling results are discussed in the next part.

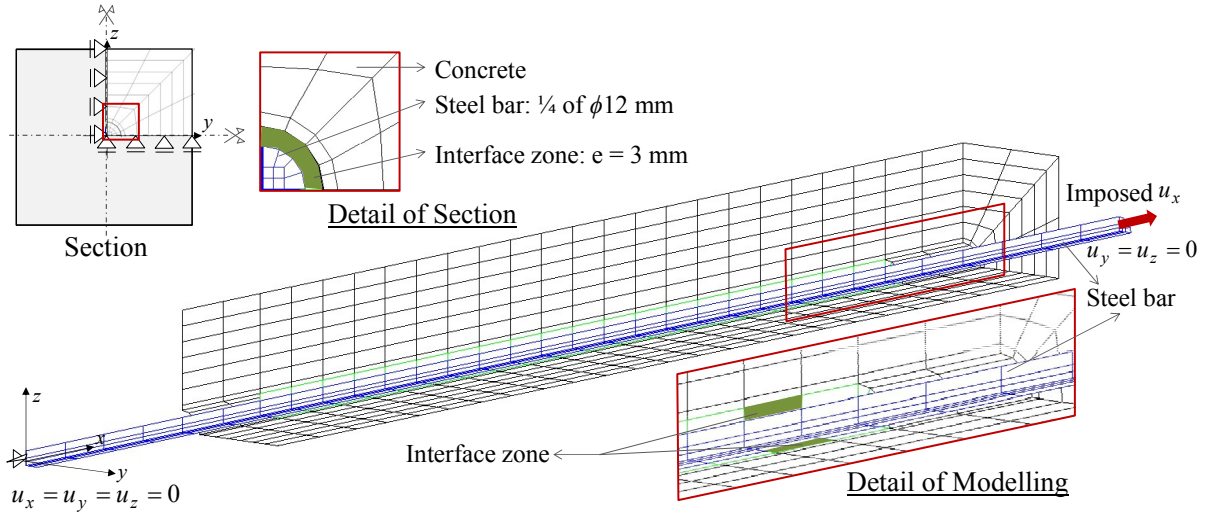


Figure 6: Mesh and boundary conditions for modelling (one fourth of specimen's volume).

4 ANALYSIS OF EXPERIMENTAL AND MODELLING RESULTS

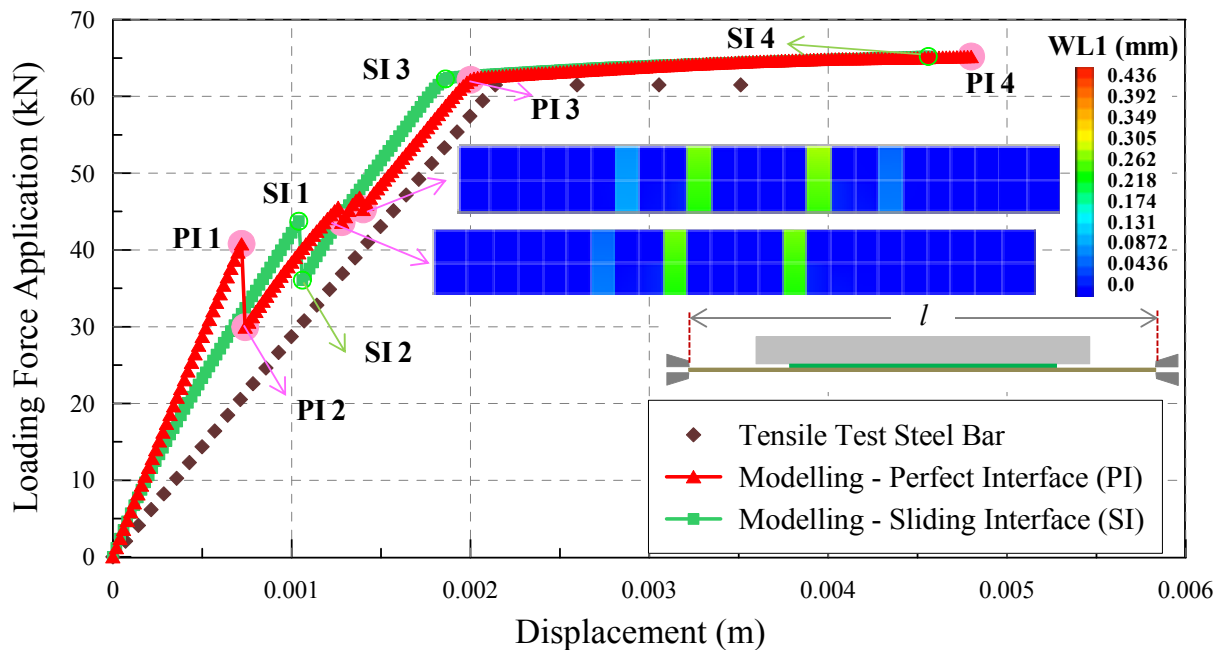


Figure 7: Force-displacement curves (global).

In this part, comparison of experimental and two modelling results are discussed.

Highlighted in four events, such as before and after first localization of crack, before strain hardening and at the maximal applied force, the comparison of two modelling and experimental results is summarized in the Table 4.

Figure 7 shows the two modelling results (PI and SI) of reinforced concrete element model compared to experimental tensile test of the steel bar alone. The difference between model's curves and steel bar behaviour represents the contribution of concrete to the RC element stiffness (tension stiffening effect). First localized crack of PI ($F = 41$ kN) appears earlier than SI ($F = 45$ kN). Before the first crack, the slope of PI is steeper than SI because of the behaviour law used in the interface zone, which is stiffer for PI than for SI.

By the reason of the observation surface using DIC, the comparison of experimental tensile prismatic element test results (ER) and two modelling results is presented in force-displacement as shown in the Figure 8. Observing the curve of force-displacement between two points on concrete surface, PI modelling results has larger displacement after the first localisation of crack than the SI results. Regarding the sum of crack opening in Figure 9 and Table 4, this large gap of displacement is due to the opening of two localized crack in the case of PI model. Comparing to Figure 7, the slope of the two curves at the beginning from modelling results show different behaviour. It seems normal since in Figure 8, only concrete surface is observed; the closer to the surface, the smaller delta displacement is, following the behaviour of interface element. In other words, as the micro crack diffuse at the beginning of the test (before the localisation crack takes place), its distribution in the case of perfect interface (PI) model is more dispersed than in case of plastic sliding interface (SI) model.

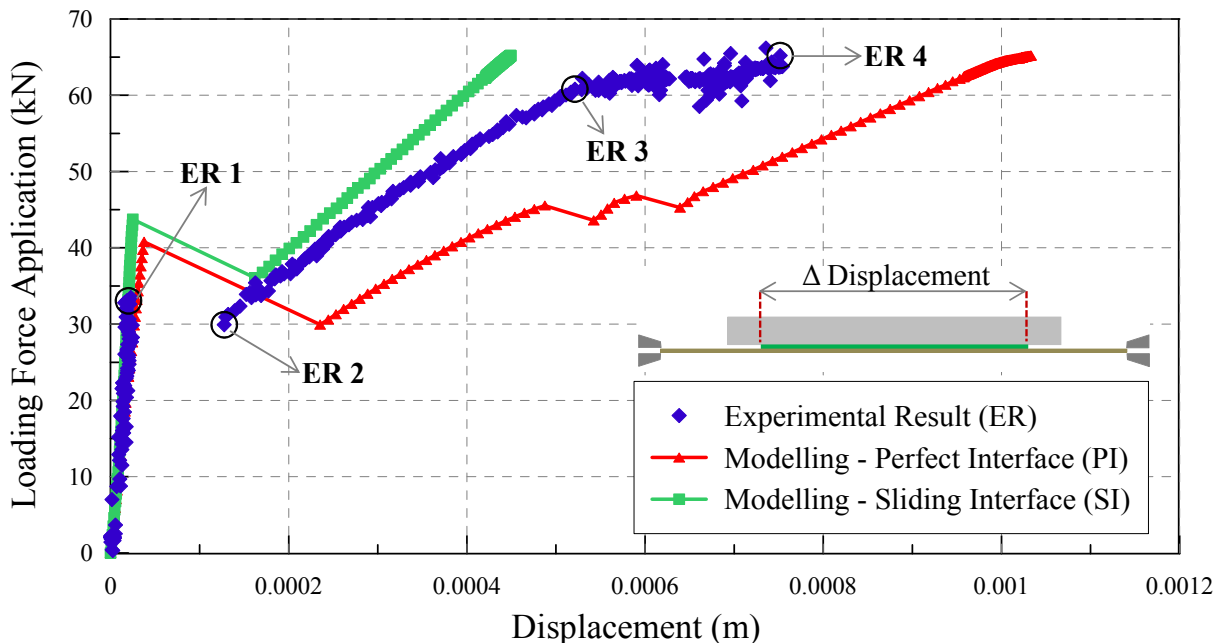


Figure 8: Force-displacement curves.

In the Figure 9, the relative displacement of two points perpendicular to the crack is shown. This relative displacement can be compared to the crack opening prediction (WL1) in Table 4. Three positions of crack were observed in order to obtain the experimental

distribution. It must be notified that the crack opening of modelling results in case of Perfect Interface (PI) corresponds to the opening of one localized crack only, not the total opening of all cracks.

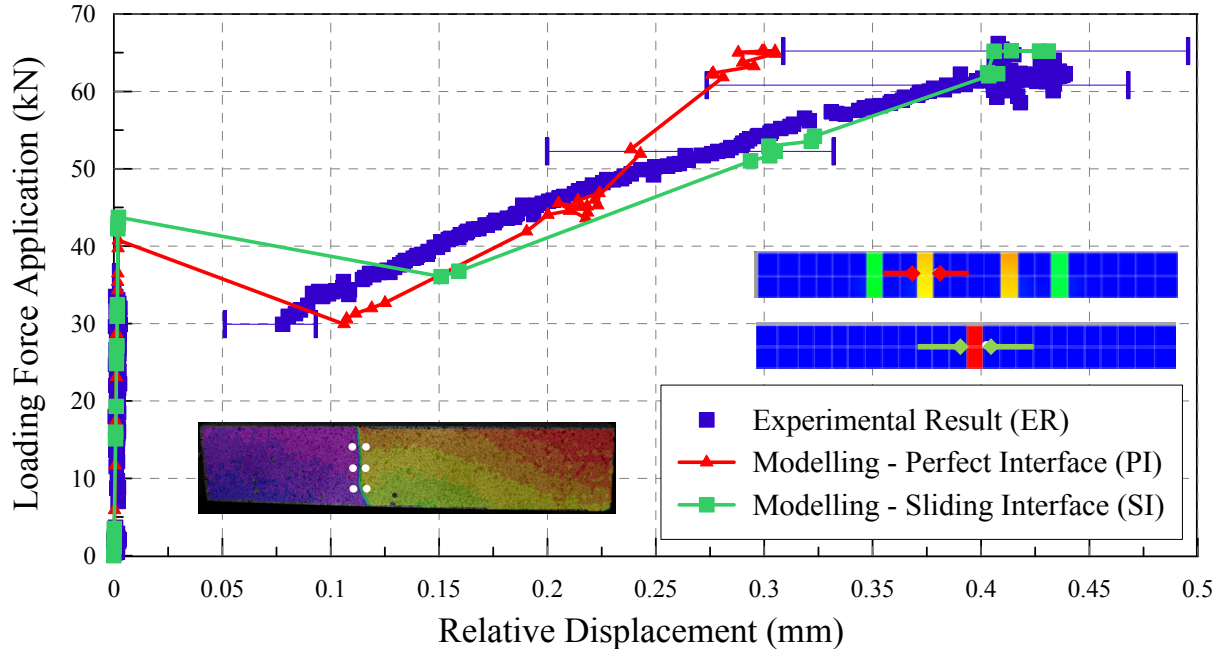














Figure 9: Force - Relative displacement of two points measuring crack opening.

According to the last figure, experimental results show approximately 0.5 mm of maximum relative displacement in x direction at the end of test. At the same value of force, the modelling results in both case of perfect and sliding interface have value close to experimental results (0.43 mm). However, PI results show four cracks while experimental results present one crack only. Therefore, it is clear that the model without sliding interface leads to an over estimation of cracks number.

5 CONCLUSION

A perfect interface (non-sliding behaviour law) consideration in modelling of this simple prismatic element tension test leads to multi cracks along the specimen. Four cracks appear at the end of the calculation, with cumulated crack opening closes to 1 mm at force 65.2 kN instead of one crack with an opening of 0.5 mm. This concludes that an interface model, for example, Eligehausen’s model [1] is absolutely needed to consider properly the sliding possibility along the interface. Otherwise, the crack number and the cumulative openings of cracks are over estimated, even with a realistic and regularized behaviour law for the concrete is used.

Table 4: Comparison of experimental and modelling results highlighted in four events.

	Modelling results		Experimental results DIC (ER)	Modelling results	
	Perfect Interface (PI) model			Sliding Interface (PI) model	
1 Exactly before the localized crack appear		WL1 (mm) 0.436 0.392 0.349 0.305 0.262 0.218 0.174 0.131 0.0872 0.0436 0.0			WL1 (mm) 0.436 0.392 0.349 0.305 0.262 0.218 0.174 0.131 0.0872 0.0436 0.0
2 Exactly after the localized crack appear		WL1 (mm) 0.436 0.392 0.349 0.305 0.262 0.218 0.174 0.131 0.0872 0.0436 0.0			WL1 (mm) 0.436 0.392 0.349 0.305 0.262 0.218 0.174 0.131 0.0872 0.0436 0.0
3 Exactly before the strain hardening reached		WL1 (mm) 0.436 0.392 0.349 0.305 0.262 0.218 0.174 0.131 0.0872 0.0436 0.0			WL1 (mm) 0.436 0.392 0.349 0.305 0.262 0.218 0.174 0.131 0.0872 0.0436 0.0
4 Maximum applied force (F = 65,2 kN)		WL1 (mm) 0.436 0.392 0.349 0.305 0.262 0.218 0.174 0.131 0.0872 0.0436 0.0			WL1 (mm) 0.436 0.392 0.349 0.305 0.262 0.218 0.174 0.131 0.0872 0.0436 0.0

REFERENCES

- [1] Eligehausen, R., Popov, E. P. and Bertero, V. V. Local Bond Stress-Split Relationships of Deformed Bars under Generalized Excitations, University of California, Report No. UCB/EERC-82/23 of the National Science Foundation, (1983).
- [2] Sellier, A., Casaux-Ginestet, G., Buffo-Lacarière, L. and Bourbon, X., Orthotropic damage coupled with localized crack reclosure processing. Part I: Constitutive Laws. *Eng Fract Mech*, (2013) **97**: 148-167.
- [3] CEOS.fr French National research project for design and assessment of special concrete structure toward cracking and shrinkage: CESOS.fr (website in French: <http://http://www.ceosfr.irex.asso.fr/en/>).
- [4] Dominguez Ramirez N. Etude de la liaison acier-béton : de la modélisation du phénomène à la formulation d'un élément fini enrichi « béton armé ». Thèse de Doctorat de l'Ecole Normale Supérieure de Cachan, (2005).
- [5] AFNOR. Steel for the reinforcement of concrete-Weldable reinforcing steel-General. NF EN 10080: 2005-09. European Standard, Published and distributed by the Association Francaise de Normalisation (AFNOR).
- [6] RILEM, Essais portant sur l'adhérence des armatures du béton: 2: Essai par traction. *Mat. Struct.* **03**: 175-178, 1970.
- [7] CAST3M-2012. <http://www-cast3m.cea.fr>
- [8] Eurocode 2, EN 1992.1.1.2004: "Design of concrete structures - Part 1-1: General rules and rules for buildings", European Committee for Standardization (CEN), Brussels, 2004.
- [9] Casanova, A., Jason, L., Davenne, L., "Bond slip model for the simulation of reinforced concrete structures", *Engineering Structures*, (2012) **39**:66-78.
- [10] Dahlblom, Ola and Ottosen, Niels Saabye, "Smearred Crack Analysis Using Generalized Fictitious Crack Model", *ASCE, J. Eng. Mech*, (1990) **116**:55-76.
- [11] Jefferson, A. D. and Bennett, T., Micro-mechanical damage and rough crack closure in cementitious composite materials, *Int. J. Num. Anal. Meth. Geomech.*(2007) **31**:133-146.
- [12] Hillerborg A., Modeer M., Petersson PE., Analysis of crack formation and crack growth in concrete by means of fracture mechanics and finite elements. *Cement and Concrete Research*, (1976) **6**:773-782.